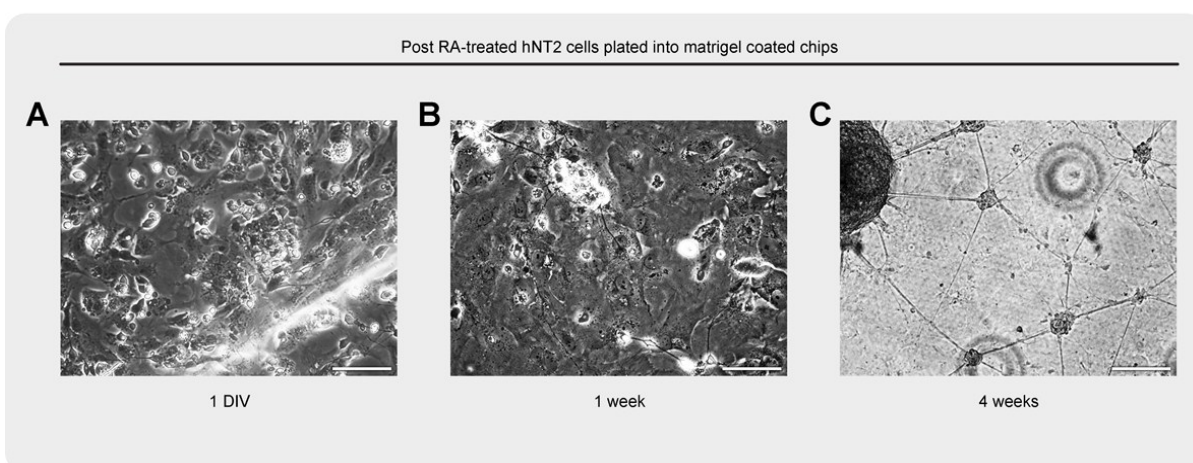
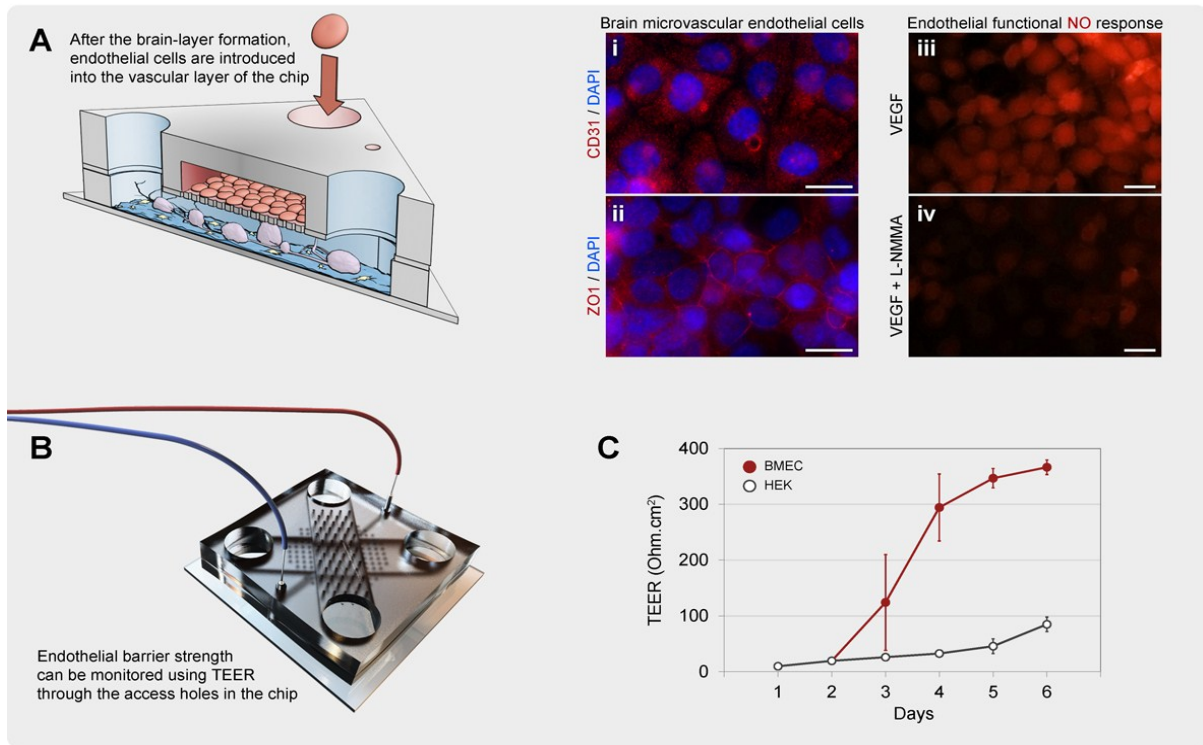


**Figure S1.** (A) Larger-area view of differentiated neuronal clusters inside the brain-on-a-chip platform, stained for mature axonal marker NF200 and mature dendritic marker MAP2ab (top). DAPI was used for nuclear staining (bottom), which reveals the non-neuronal cells interspersed between the neuronal clusters (scale bars = 500  $\mu\text{m}$ ). (B) Electrical activity of hNT2 cells cultured in a monolayer, recorded as mean of firing rates (MFR) for up to 8 weeks after RA treatment using Multi Channel Systems chips (Reutlingen, Germany) with 60 electrodes of 30  $\mu\text{m}$  diameter and 200  $\mu\text{m}$  inter-electrode spacing with an integrated reference electrode ( $n = 3$ , mean + s.e.m). MEA chips were sterilized before Matrigel (BD) and Poly-d-Lysine hydrobromide (SigmaP1149) coating.



**Figure S2.** Brightfield images showing how the morphology of RA-treated hNT2 cells changes over time while differentiating and maturing inside the brain-chips (scale bars = 200  $\mu\text{m}$ ).



**Figure S3.** Formation and characterization of an endothelial layer introduced to the top chamber of the brain-chips to mimic the blood-brain barrier (scale bars = 20  $\mu\text{m}$ ).

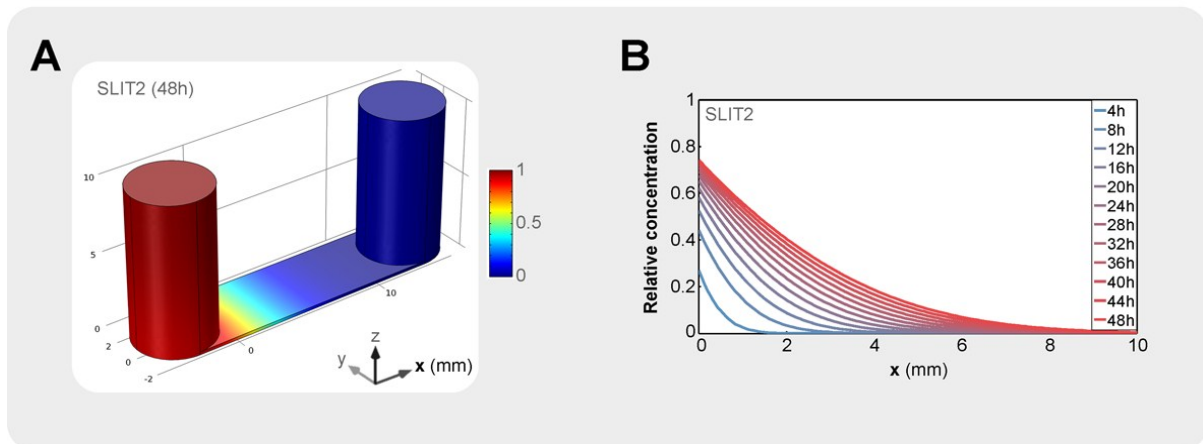


**Figure S4.** Finite-element simulation of gradient evolution in the brain chips for SLIT2 (A-B).

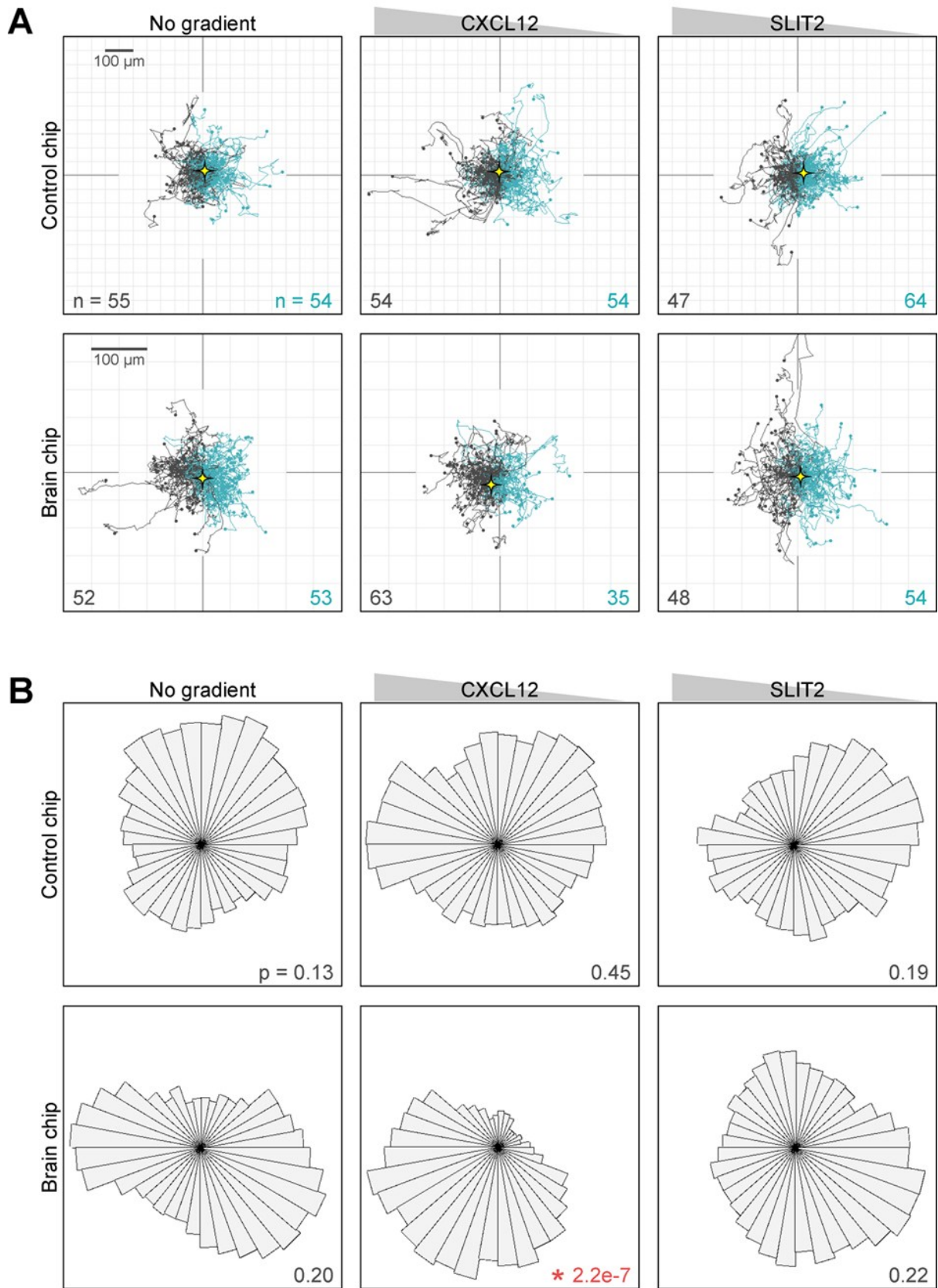


**Figure S5.** (A) hNPC cell tracks, colored based on whether the endpoints are closer or further away from the chemotactic gradient source compared to the starting points. The number of cells on each side is shown. The yellow stars denote the center of mass of the endpoint positions. (B) Angular histograms of cell endpoint positions. The Rayleigh p-value of each endpoint distribution is displayed, showing that the hNPCs respond to the CXCL12 gradient only in the presence of the brain layer.